Article

Latent Thermal Energy Storage System for Heat Recovery between 120 and 150 °C: Material Stability and Corrosion [†]

Yasmine Lalau [1,2,*], Sacha Rigal [1], Jean-Pierre Bédécarrats [1] and Didier Haillot [3,*]

[1] Universite de Pau et des Pays de l'Adour, E2S UPPA, LaTEP, 64000 Pau, France; jean-pierre.bedecarrats@univ-pau.fr (J.-P.B.)

[2] Université de Toulouse, IMT Mines Albi, CNRS UMR 5302, Centre RAPSODEE, Campus Jarlard, CEDEX 09, 81013 Albi, France

[3] Département de Génie Mécanique, École de Technologie Supérieure, 1100, Rue Notre-Dame Ouest, Montréal, QC H3C1K3, Canada

[*] Correspondence: yasmine.lalau@mines-albi.fr (Y.L.); didier.haillot@etsmtl.ca (D.H.)

[†] This paper is an extended version of our conference proceeding published in Annales du Congrès Annuel de la Société Française de Thermique 2020, Tome 1, Strasbourg, France, 9–12 June 2020, pp. 145–152.

Abstract: Thermal energy represents more than half of the energy needs of European industry, but is still misspent in processes as waste heat, mostly between 100 and 200 °C. Waste heat recovery and reuse provide carbon-free heat and reduce production costs. The industrial sector is seeking affordable and rugged solutions that should adapt the heat recovery to heat demand. This study aims to identify suitable latent heat materials to reach that objective: the selected candidates should show good thermal performance that remains stable after aging and, in addition, be at a reasonable price. This paper details the selection process and aging results for two promising phase change materials (PCMs): adipic and sebacic acid. They showed, respectively, melting temperatures around 150 °C and 130 °C, degradation temperatures (mass lost higher than 1%) above 180 °C, and volumetric enthalpy of 95 and 75 kWh·m^{-3}. They are both compatible with the stainless steel 316L while their operating temperature does not exceed 15 °C above the melting temperature, but they do not comply with the industrial recommendation for long-term use in contact with the steel P265GH (corrosion speed > 0.2 mm·year^{-1}).

Keywords: thermal energy storage; heat recovery; phase change materials; calorimetry; corrosion

1. Introduction

The continuous increase in the level of greenhouse gas emissions and the reduction in production costs are the main driving forces to encourage all stakeholders in the manufacturing sector to improve the energy efficiency of their production processes. In fact, at the present time, a large amount of energy is rejected at a low temperature level (between 0 and 150 °C). For instance, in France, the amount of industrial energy losses below 200 °C is estimated to be 83 TWh·year^{-1}, representing 75% of the total heat wasted by the French industry [1]. At the EU level, the waste heat potential is about 300 TWh·year^{-1}, with one-third corresponding to temperature levels below 200 °C [2]. According to the US Department of Energy (DOE), a barrier to massive heat recovery at low temperature levels is the lack of end uses that should be enlarged by introducing efficient heat storage solutions [3]. One option is to recover energy from the waste stream using thermal energy storage (TES) technology, including phase change material (PCM) [4]. This technology appears particularly attractive compared to sensible or thermochemical heat storage since it offers the best compromise between a sufficient Technology Readiness Level (TRL) and a high-energy storage density, facilitating the system's integration in a complex industrial environment. Additionally, it provides an almost constant temperature, avoiding process disturbances or increasing the performances, for example, when the TES is combined with an Organic Rankine Cycle (ORC) [5,6].

These arguments led to the development of a storage system containing a PCM melting at a temperature included in the 120–150 °C range. This temperature range corresponds to the pre-heating of existing industrial processes. Many types of heat exchangers can be utilized [5]. The use of a shell and tube heat exchanger seems a relevant option because this technology is widely used in industry. Specifically, a multi-tubular heat exchanger is considered where the PCM is located in the shell, around the tubes (Figure 1). The shell acts as an envelope for the PCM, preventing its leakage, when it is in a liquid state.
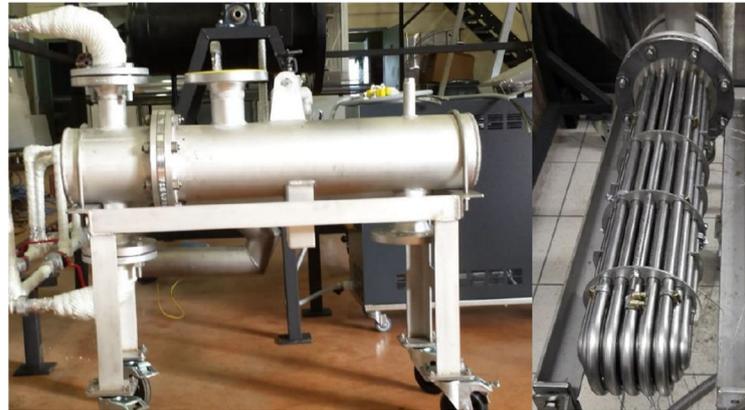
Figure 1. Types of exchanger planned to contain the PCM.

Among the different energy storage technologies presented in Figure 2, the thermal one is considered in this study. The developed TES system involves PCMs whose storage capacity corresponds to their latent heat. The liquid-to-vapor transition shows the greater enthalpy, but is associated with high volumetric expansion, requiring consequent volumes and/or high-pressure tanks. This expansion is negligible in solid–solid transition, but the transition kinetic is generally too slow and associated with low enthalpies. The solid–liquid transition is preferred for both its intermediate latent heat and thermal expansion.
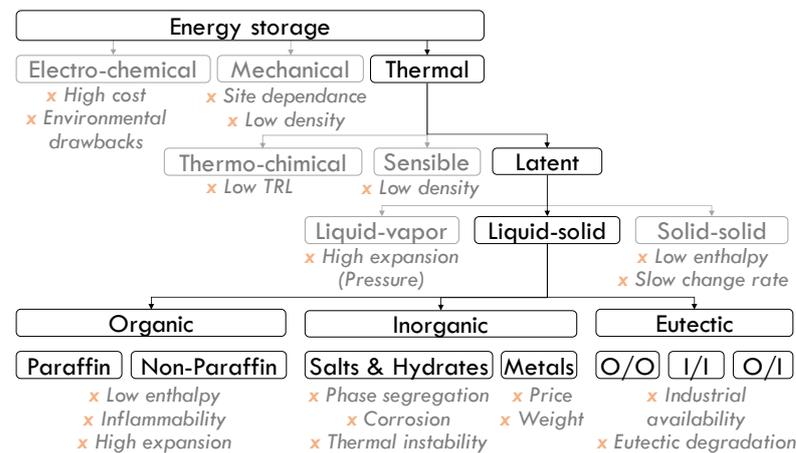
Figure 2. Energy storage families and their main drawbacks (red crosses).

PCMs are classified into two distinct families: organic and inorganic materials [7]. This classification can be completed by incorporating eutectics, which can be a mixture of organic and inorganic compounds.

Organic materials [8] can be classified into two categories: paraffins and non-paraffins. Paraffins are by-products of petroleum distillation and belong to the alkane family. They are molecules with an empirical formula of C_nH_{2n+2} and structural formula of $CH_3\text{-}(CH_2)_n\text{-}CH_3$. One of the main properties of these materials is that the longer the carbon chain is, the higher its melting temperature. Paraffins are non-toxic, chemically stable and inert below 500 °C. Their supercooling degree (the difference between the melting and crystallization

temperatures) is generally low. However, it should be noted that they have a relatively low thermal conductivity ($0.2\ W \cdot m^{-1} \cdot K^{-1}$) and a volume expansion during phase changes of up to 15%. A high thermal conductivity increases the heat transfers and provides high thermal storage\discharge power, and a low thermal expansion coefficient avoid mechanical stress on the PCM envelope. The non-paraffin subgroup is the largest group of PCMs in the literature, as it is composed of several subfamilies, including fatty acids and sugar alcohol polyols. Fatty acids, having a general formula of $C_mH_nO_2$, have been widely used because of their good thermo-physical properties: high thermal capacity, good thermal and chemical stability, non-toxic, non-corrosive, low degree of supercooling and low cost. However, they are flammable, have low thermal conductivity, have different levels of toxicity, and are unstable at high temperatures. Polyols are compounds with an empirical formula of $(CHOH)_nH_2$. These materials are increasingly studied because their melting temperature can be between -15 and $245\ ^\circ C$ and their enthalpy change may be up to $413\ J \cdot g^{-1}$, with a density often exceeding $1500\ kg \cdot m^{-3}$ [9]. Moreover, these PCMs are non-toxic and non-hazardous to humans and the environment. However, they have a high degree of supercooling [10] and a volume expansion at phase change of up to 15%.

The inorganic group is mainly composed of salts or hydrated salts and metals [11]. Metals have a melting point much higher than the temperature range required for this study. Hydrated salts contain water and are characterized by the general formula $M_xN_y.nH_2O$. Although hydrated salts have high volume enthalpy of phase change, good thermal conductivity and low volume expansion during phase transformation, their melting is very often incongruous (segregation). The transformation is thus incomplete and by difference in density, there can be a separation of several components. It is also possible to note a tendency of supercooling. Salts are pure bodies of ionic structure formed from anions and cations. These materials have properties similar to hydrated salts; however, the absence of the water molecule allows their use at higher temperatures.

In addition to these general characteristics, PCMs in the same family can also differ according to physical, chemical, and economic criteria that are important for industrial applications. The first part of this paper is dedicated to the screening and selection of the most suitable PCM for our application: waste heat recovery between 120 and 150 $^\circ C$.

There is another important constraint to bear in mind. The selected PCM is meant to be used in a metallic heat exchanger, and should thus be compatible with long-term use within this envelope. Corrosion implies serious drawbacks, such as making the metal brittle and threatening a structure collapse. It could also modify the PCM's properties, degrading its thermal performances or increasing its viscosity and thus the operational pumping costs [12]. Viscosity increase is not an issue in this work as the PCM is stacked in the heat exchanger and does not circulate. The corrosion issue has been studied over a wide range of temperatures, from cold applications [13–15] to high temperatures [16], especially for concentrated solar power applications and thus with molten salts used as PCMs [17–19], passing the building temperature level [20–22]. Fewer studies have focused on the medium temperature range that concerns us (120–150 $^\circ C$) [23]: a recent paper investigated the compatibility between a commercial PCM named PlusIce S83 (mainly composed of magnesium nitrate) with aluminum, copper, and carbon steel [24]. Those previous works demonstrate the importance of such studies. The second part of this paper is dedicated to the stability and corrosion behavior of industrial-grade PCMs.

Previous works have already been carried out to select and characterize PCMs in the temperature range between 120 and 150 $^\circ C$. However, not all the works have considered material stability and possible corrosion problems. In addition, the results obtained by the authors may differ from one publication to another. The aim of our work was to specify the properties of materials that have already been identified and studied in the literature, and also to select new ones potentially.

2. Phase Change Materials Screening and Selection

2.1. Selection Criteria

The first criterion to choose an appropriate PCM is its transition temperature: in the present study, the focus was on the 120–150 °C range. The selection also considers the following features [25,26]:

- Physical: besides the suitable transition temperature, the PCM should have:
  - High volumetric enthalpy (high latent heat and high density) to provide high-density storage. The value of 50 kWh·m^{-3} was taken as a reference. It corresponds to the variation enthalpy of water in a temperature range of approximately 0–43 °C;
  - High thermal conductivity to increase the heat transfer and provide high thermal storage\discharge power (may be optimized by the system geometry);
  - Low thermal expansion coefficient to avoid mechanical stress on PCM envelope;
  - Good phase equilibrium (no segregation during phase change), as phase segregation during transition disrupt heat transfer and can be partially irreversible;
  - No supercooling that delays crystallization.

- Chemical:
  - Long-term chemical stability to avoid performance degradation through thermal cycling;
  - Compatibility with enveloping materials to avoid corrosion;
  - No toxicity nor fire hazards.

- Economics:
  - PCM should be industrially available in large quantities;
  - For a cost-effective storage system, the PCM price should remain affordable. This is highly dependent on the targeted application: for a short-term storage (about 3 cycles per day), the International Renewable Energy Agency (IRENA) estimated a viable investment cost at 225 EUR·KWh^{-1} for the whole system [27]. Accounting for approximately 45% of this investment for the phase change material [28], its cost should remain under 100 EUR·KWh^{-1}.

2.2. Materials Screening

The literature review selected the organic PCMs whose melting temperature is included in the targeted range (120–150 °C), as referenced in Table 1 [29]. This table also gives their density ρ, their latent heat ΔHm, and their volume enthalpy variation ΔHm,vol. A price estimation range is given based on ΔHm,vol: <50 EUR·KWh^{-1} (+ + +), <100 EUR·KWh^{-1} (+ +), <150 EUR·KWh^{-1} (+), <500 EUR·KWh^{-1} (-), < 1000 EUR·KWh^{-1} (- -), and >1000 EUR·KWh^{-1} (- - -). This is a rough criterion that does not include the sensible part of the storage (would increase ΔHm,vol) nor the system envelope and porosity (would decrease ΔHm,vol).

Three PCM classes were ruled out in this study:

- Metals, for their high costs. Two PCMs fit in the temperature range [30]: Indalloys 255 (55.5%mBi + 44.5%mPb, toxic) and 281 (58%mBi + 42%mSn), with the respective melting temperatures of 125 °C and 138 °C. They show a similar volume enthalpy variation to organic PCMs (respectively, 58 and 107 kWh·m^{-3}), but their thermal conductivity is ~100 higher, supporting higher power.
- Eutectics, for their complex industrial production which hinders a precise and stable eutectic. Five PCMs could have been selected for their melting temperature [17,31]: 30%mLiNO$_3$ + 18%mNaNO$_3$ + 52%mKNO$_3$ (120 °C), 33%mLiNO$_3$ + 67%mKNO$_3$ (125 °C), 38.2%mLiNO$_3$ + 61.8%mCO(NH$_2$)$_2$ (125 °C), 44%mCa(NO$_3$)$_2$ + 44%mNaNO$_3$ + 12%mKNO$_3$ (140 °C), and 40%mNaNO$_2$ + 7%mNaNO$_3$ + 53%mKNO$_3$ (142 °C).
- Inorganics, whose candidates in the focused range [31,32] were industrially unavailable (ammonium zinc sulfate hexahydrate and magnesium nitrate dihydrate,

T_m = 125 °C and 130 °C, respectively), or suffered early damage (sodium acetate trihydrate, T_m = 137 °C).

Among the 32 remaining candidates, several were removed for the following reasons [31–34]:

- High cost (- -): mandelic acid, valporic acid, suberic acid, methyl-4'-acetanilide [30], chlorobenzoic acid, and xylose-L;
- Early damage (decomposition temperature closer than 20 °C to the melting temperature): urea, malonic acid, maleic acid, DL-malic acid, trans cinamic acid, fructose-D, and glucose-D;
- Enthalpy variation lower than 50 kWh·m^{-3}: HDPE [35], stilbene, and trans-1,4-polybutadiene [6];
- Hazardousness (flammability, toxicity): picric acid, benzamide, phenacetine, and anthranilic acid;
- Significant supercooling (more than 30 °C): erythritol (despite a very attractive latent heat) and tromethanol (in addition to a high cost) [36].

Some polyols could be of interest: maltitol, isomalt [37], xylose-D, and lactitol. However, the first two decomposed during their first thermal cycling and the last two were not industrially available when this study started.

Finally, six PCMs were selected for thorough examination: succinic anhydre acid, benzoic acid, phtalic anhydre [38], sebacic acid [39], dimethyl terephtalate, and adipic acid.

Table 1. PCM candidates for latent heat storage in the range 120–150 °C, the 6 selected are in bold. * [31–34] <50 EUR·KWh^{-1} (+ + +), <100 EUR·KWh^{-1} (+ +), <150 EUR·KWh^{-1} (+), <500 EUR·KWh^{-1} (-), < 1000 EUR·KWh^{-1} (- -), and >1000 EUR·KWh^{-1} (- - -). Reprinted with permission from Y. Lalau, D. Haillot, S. Rigal, J.-P. Bedecarrats (2020), copyright 2020 Société Française de Thermique [29].

Name	Formula	ρ [kg·m^{-3}]	T_m [°C]	ΔH_m [kJ·kg^{-1}]	$\Delta H_{m, vol}$ [kWh·m^{-3}]	N° CAS	Price [EUR kWh^{-1}]	Comments	Ref
Erythritol	$C_4H_{10}O_4$	1480	118–120	340	140	149-32-6	+ + +	Supercooling > 80 °C	[36]
Succinic anhydride acid	**$C_4H_4O_3$**	**1560**	**118–121**	**206**	**89**	**108-30-5**	**+ +**		*
Mandelic acid	$C_6H_5CH(OH)CO_2H$	1300	118–121	161	58	90-64-2	- -	High cost	[30]
Valporic acid	$C_8H_{16}O_2$	904	120	203	51	99-66-1	- -	High cost	[30]
Benzoic acid	**$C_7H_6O_2$**	**1266**	**121.7**	**143**	**50**	**65-85-0**	**+ +**	**Supercooling: 22 °C**	*
Picric acid	$C_6H_3N_3O_7$	1760	122	75	37	88-89-1		Flash point 150 °C, explosive	*
HDPE	$(C_2H_4)n$	940	125	167	44	9002-88-4		Enthalpy < 50 kWh·m^{-3}	[35]
Stilbene	$C_{14}H_{12}$	970	126	167	45	103-30-0		Enthalpy < 50 kWh·m^{-3}	*
Benzamid	C_9H_7NO	1341	127.2	169	63	55-21-0		Toxic	*
Tromethamine/Tromethanol	$C_4H_{11}NO_3$	1353	131	285	107	77-86-1	-	Supercooling: 66 °C, High cost	[36]
Anydride phthalic	**$C_8H_4O_3$**	**1530**	**131**	**159**	**68**	**85-44-9**	**+ + +**	**Supercooling: 23 °C**	[38]
Sebacic acid	**$C_{10}H_{18}O_4$**	**1209**	**131–133**	**243**	**82**	**111-20-6**	**+ +**		[39]
Maleic acid	$C_4H_4O_4$	1590	131–140	235	104	110-16-7		Decomposition ~145 °C	*
DL- malic acid	$C_4H_6O_5$	1601	131–140	225	100	6915-15-7		Decomposition ~150 °C	*
Urea	$CO(NH_2)_2$	1323	132	251	92	57-13-6		Low stability	*
Malonic acid	$C_3H_4O_4$	1620	132–136			141-82-2		Decomposition ~135 °C	*
Trans cinnamic acid	$C_9H_8O_2$	1250	133	153	53	140-10-3		Decomposition ~146 °C	*
Phenacetin	$C_{10}H_{13}NO_2$	1240	134	175	60	62-44-2		Toxic	*
Chrolobenzoic acid	$C_7H_5ClO_2$	1540	140	164	70	118-91-2	- -	High cost	*
Suberic acid	$C_8H_{14}O_4$	1020	141–144	245	69	505-48-6	- -	High cost	[30]
Dimethyl terephtalate	**$C_{10}H_{10}O_4$**	**1290**	**142**	**170**	**61**	**120-61-6**	**+ +**		*
Fructose-D	$C_6H_{12}O_6$	1690	144–145	145	68	57-48-7		Early degradation	*
Isomalt	$C_{12}H_{24}O_{11}$	1040	145	170	71	64519-82-0	-		[37]
Trans-1,4-polybutadiene (TPB)	C_4H_6	1010	145	144	40	25038-44-2		Enthalpy < 50 kWh·m^{-3}	[6]
Maltitol	$C_{12}H_{24}O_{11}$	1620	145–152	173	78	585-88-6	+ + +		*
Methyl-4'-acetanilide	$C_9H_{11}NO$	1370	146–151	180	69	103-89-9	- - -	High cost	[30]
Lactitol	$C_{12}H_{24}O_{11}$	1690	146–152	135–149	70	585-86-4	+ + +	Industrial availability	*
Anthranilic acid	$C_6H_4(NH_2)COOH$	1410	147	148	58	118-92-3		Flash point 150 °C	*
Xylose-D	$C_5H_{10}O_5$	1525	147–151	216–280	118	58-86-6	+ + +		*
Xylose -L	$C_5H_{10}O_5$	1525	147–151	213	90	609-06-3	- - -	High cost	*
Glucose -D	$C_6H_{12}O_6$	1540	149–152	180	82	50-99-7		Low stability	*
Adipic acid	**$C_6H_{10}O_4$**	**1360**	**151–155**	**260**	**98**	**124-04-9**	**+ + +**		*

2.3. Calorimetric Analysis

Calorimetric analysis performed by differential scanning calorimetry (DSC) and the T-history method [40] were the main methods used to obtain the storage capacity of PCMs. DSC was used because it is fast and available in the laboratory. These measures were coupled with thermogravimetry. The results are presented after the description of the operating method.

2.3.1. Material & Method

Differential Scanning Calorimetry (DSC)

The calorimetry measurements were performed in hermetic (21 bars) 60 µL cells thanks to a power-compensation calorimeter (Perkin Elmer Pyris Diamond). Once filled with PCM (~20 mg), the cells were sealed with a press. They were weighted by a Mettler Toledo XP26 scale with a 0.002 mg precision, resulting in an uncertainty of measurement of 0.004 mg (empty and filled cells).

Those measurements allow both the melting temperature and phase change enthalpy variations to be obtained, as well as information regarding the thermal cycling behavior of the selected materials. In order to reduce the characterization duration, $20\ °C \cdot min^{-1}$ cooling and heating rates were applied between 30 °C under and above the melting temperature, as presented in Figure 3. The 38th and 75th cycles were compared to the 2nd, which was taken as the reference value.
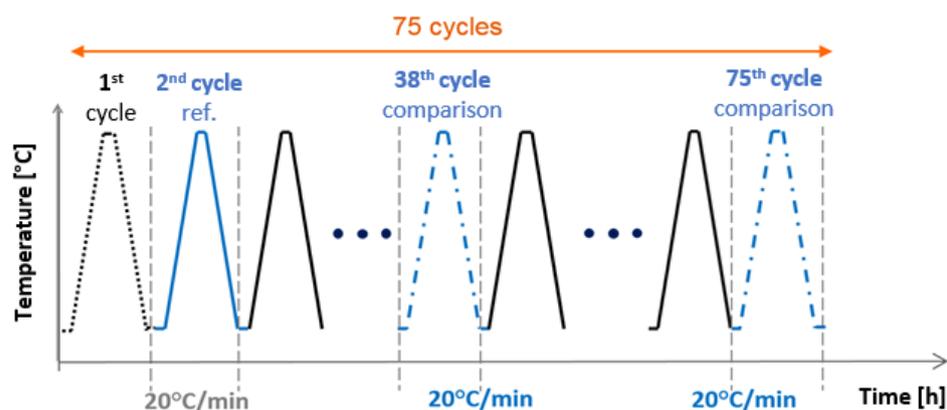
Figure 3. Thermal cycling for PCM stability test.

Using DSC, the melting temperature T_m was graphically determined by the onset method, as illustrated in Figure 4 [41], and then named T_{onset}. A crystallization temperature was also defined by this method, allowing us define the criteria ΔT_{mean}, which is the difference between the melting and the crystallization temperature.

This high-speed heating rate allowed us to reduce the characterization duration to verify the materials' properties compared to the literature and to roughly determine their thermal stability through a high number of cycles. The finest characterization of the ultimately selected materials (Section 3) was performed at a reduced heating rate of $2\ °C \cdot min^{-1}$.

Thermogravimetry Analysis (TGA)

The thermogravimetry analysis gives the PCMs' mass loss when submitted to an unusual temperature increase in order to quantify their maximum usable temperature within the TES system.

The selected PCMs were placed in an alumina crucible, weighted with the same scale used for DSC tests, and tested under air as gas purge in 170 µL in the Setsys Cryostat from Setaram (Caluire-et-Cuire, France).

Each sample (~100 mg) was submitted to the following temperature profile:

- A 10 min isothermal step at 35 °C below the melting temperature;

- A 2 °C·min^{-1} slope up to 100 °C above the melting temperature.

The irreversible damage threshold was defined at the temperature T1% where the PCM loses 1% of its initial mass. To be used safely in industrial conditions, the difference between the melting temperature and this degradation temperature T1% should be sufficient (greater than 20 °C as order of magnitude).
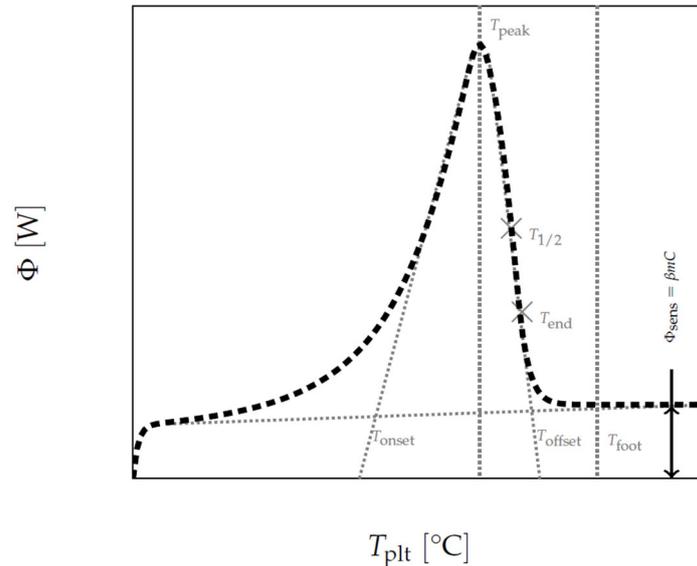
Figure 4. Example of a thermogram with the corresponding characteristic temperatures. Reprinted with permission from Stéphane Gibout, Erwin Franquet, Didier Haillot, Jean-Pierre Bédécarrats, and Jean-Pierre Dumas (2018), copyright 2018 Applied Science [41].

2.3.2. Results and Analysis

The DSC heating and cooling curves are provided for two of the studied PCMs in Figure 5a adipic acid and Figure 5b sebacic acid. For both of them, a small evolution appeared between the reference cycle (2nd cycle) and the 38th cycle, but the sample behavior seems have stabilized between the 38th and 75th cycle.

(**a**) adipic acid
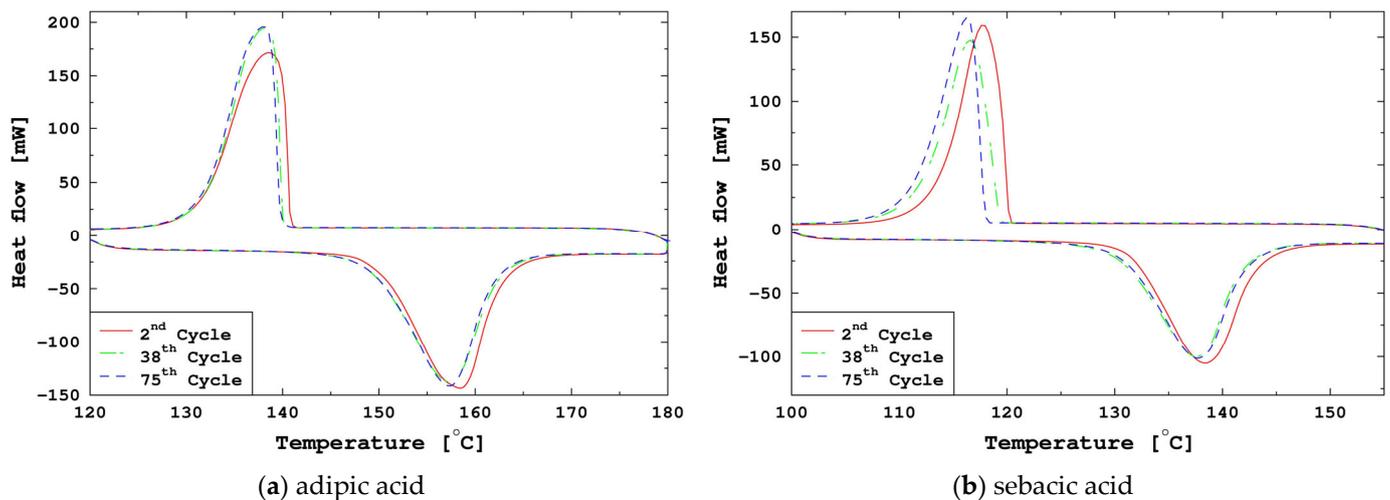
(**b**) sebacic acid

Figure 5. DSC heating and cooling curves for (**a**) adipic acid and (**b**) sebacic acid.

The mass loss profiles from thermogravimetric analysis are illustrated in Figure 6a for adipic acid and Figure 6b sebacic acid. For both of them, their mass remains stable up to approximately 180 °C, reaching a 1% mass loss at, respectively, 186.1 °C and 181 °C. This threshold is 35 °C and 51 °C above their respective melting temperatures.

(**a**) adipic acid
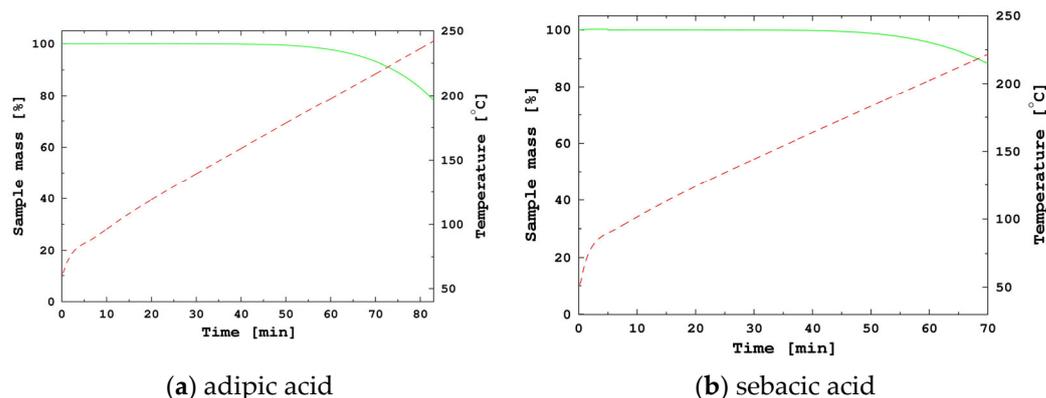
(**b**) sebacic acid

Figure 6. Sample mass loss profiles (green continuous line, left axis) and temperature (red dotted line, right axis) from TGA for (**a**) adipic acid and (**b**) sebacic acid.

The measurement results on selected materials are synthetized in Table 2.

Table 2. Thermal characterization synthesis of PCM candidates (grey boxes enlighten values below the targeted performances).

	DSC (2nd, 38th, and 75th Cycles)							TGA
	T_{onset} [°C]			$\Delta H_{m, vol}$ [kWh·m^{-3}]			ΔT_{mean} [°C]	$T_{1\%}$ [°C]
Precision	±0.4 °C			±1.3%			±0.4 °C	-
Succinic anhydride	115.3	115.7	115.3	77.6	74.5	71.9	60.8	115.7
Benzoïque acid	121.5	120.5	120.7	49.6	47.1	46.4	25.0	122.4
Phtalic anhydride	129.1	128.9	129	65.9	60.4	58.7	27.3	124.0
Sebacic acid	**131.5**	**130.3**	**130.8**	**75**	**70**	**71**	**11.7**	**181.0**
Dimethyl terephtalate	140.2	139.9	140.4	58.4	54.8	53.4	9.7	128.7
Adipic acid	**150.0**	**149.1**	**149.6**	**95.2**	**92.6**	**92.2**	**10.0**	**186.1**

According to the DSC analysis, the melting temperatures are consistent with the literature and remain stable along the thermal cycles, except for succinic anhydride, which melted at 115 °C instead of 118–121 °C, excluding this candidate from the focused temperature range, i.e., 120–150 °C.

Even if DSC gives information on supercooling PCM behavior, a specific value cannot be determined, as the supercooling phenomenon is mainly dependent on the sample volume [36], which is not representative of industrial system volumes. However, although the supercooling decreased with the increase in the volume, the DSC test revealed a potential issue with the succinic anhydride (ΔT_{mean} = 60.8 °C) and to a lesser extent with the phtalic anhydre (ΔT_{mean} = 27.3 °C) and the benzoic acid (ΔT_{mean} = 25 °C).

A slight decrease (generally less than 5%) was observed between the literature and the measured values of latent melting heat [31–34,38,39], with a more noteworthy difference for sebacic acid (8.5%) and succinic anhydride (12.5%). During the thermal cycling, this latent heat showed a decrease above 5% for succinic anhydride, phtalic anhydride, dimethyl terephthalate, and benzoic acid, and up to 11% between the 2nd and 75th phtalic anhydride cycles. This performance degradation could be detrimental to industrial uses involving melting/crystallization repeated phases and should be considered in the system design.

This critical stability was evaluated by thermogravimetry analysis: the four PCMs lost more than 1% in mass at a temperature close to, or even below, the melting temperature, leading to a complete sample evaporation at the end of the test. This degradation being incompatible with the industrial use, those materials are removed from the study.

Only two candidates were ultimately selected: sebacic acid and adipic acid. To confirm their suitability, their property stability had to be studied. In order to analyze their real performances, the following stability and corrosion studies were conducted in industrial grade materials provided by Altichem® (Saint-Ouen-l'Aumône, France).

3. Stability and Corrosion Study

3.1. Materials and Method

3.1.1. Stability Study: PCM Thermal Aging

The stability study aimed to observe PCM behavior when exposed to higher temperatures than the standard conditions. This could happen during monitoring failures, and should not deteriorate the PCM's thermophysical properties. It is also a way to ensure that the properties of the material remain stable over time despite the multiple cycles of temperature rise and fall.

The PCMs were exposed to two-month thermal aging in three stoves at a specific temperature. Each stove contained as many hermetically sealed bottles as samples to characterize by DSC at the given frequency: 1 day, 2 days, 4 days, 8 days, 16 days, 30 days, and 60 days. The stove temperatures were set to 15 °C, 25 °C, and 35 °C above the PCM melting temperature (respectively, T1, T2, and T3). The DSC measurements were performed by the same apparatus as presented in the previous paragraph, but at a reduced speed (2 °C·min^{-1}), and only three cycles were performed to obtain a mean value of T$_{onset}$ and ΔH_m.

3.1.2. Corrosion Study: PCM and Envelope Thermal Aging

In the corrosion study, a piece of the materials used for the storage system envelope was added to the sealed bottles, and the same thermal aging protocol as for the stability study was followed. The DSC measurement controls the influence of the envelope material on the PCM properties, and an observation coupled with the weight of the envelope material gives information on its corrosion by the PCM.

This study took place in an industrial research project where the TES consisted of a shell and tube heat exchanger (HX) filled with the PCM. The intended HX was made of 361L stainless steel (tubes) and P265GH steel (shell). These material samples were submerged in the liquid PCM, and had the following size: a 30 × 12 mm^2 surface for both and thicknesses of 0.5 mm and 4 mm, respectively, for 316L and P265GH. The steel sample mass differences before and after aging were measured to calculate the corrosion speed v_{corr} according to ASTM G01 norms [42].

$$v_{corr} = \frac{K \times \left(m_i - m_f \right)}{S \times \Delta t \times \rho} \tag{1}$$

where K = 87,600, a unit converter coefficient (from cm·h^{-1} to mm·year^{-1}), S is the total surface sample in cm^2, Δt is the experiment duration in h, ρ is the metal density in g·cm^{-3} and m_i, and is m_f the initial and final sample mass in g. According to Table 3, the corrosion speed should not exceed 0.02 mm·year^{-1} to be economically viable for industrial use.

Table 3. Industrial guide for corrosion mass loss acceptance [14,43].

Corrosion Speed [mm·Year^{-1}]	Recommendations
>2	Completely ruined in a few days
0.2–2	Not recommended for use longer than one month
0.1–0.2	Not recommended for use longer than one year
0.02–0.1	Use carefully depending on conditions
<0.02	Long-term use

3.2. PCM Thermal Aging

The T_{onset} evolution is illustrated in Figures 7 and 8, respectively, for adipic and sebacic acid, while Figures 9 and 10 describe the latent melting heat evolution for the same materials. The initial values were $T_{onset} = 152\ °C$ and $\Delta H_m = 240\ kJ \cdot Kg^{-1}$ for adipic acid and $T_{onset} = 131\ °C$ and $\Delta H_m = 224\ kJ \cdot Kg^{-1}$ for sebacic acid. The temperatures T1, T2, and T3 were, respectively, 15, 25, and 35 °C above the PCM onset temperature. The small variations (~1% for T_{onset} and ~5% for ΔH_m) did not reveal a downward tendency over the two months studied, neither for adipic nor sebacic acid; the materials should therefore be suitable for long-term use as thermal storage materials in the targeted temperature range. Thus, the compatibility study with the storage envelope was relevant for both materials.
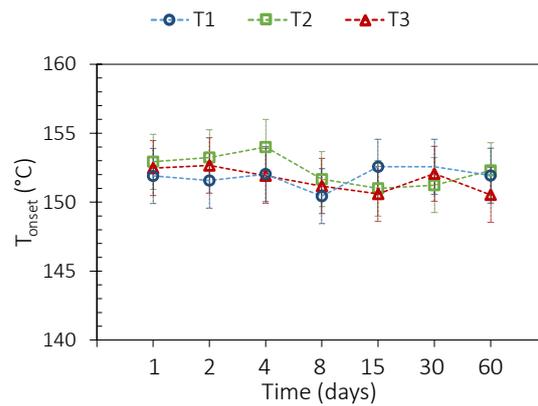
Figure 7. T_{onset} variation of adipic acid.
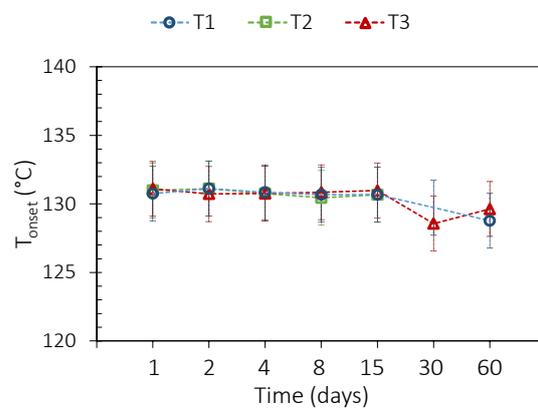
Figure 8. T_{onset} variation of sebacic acid.
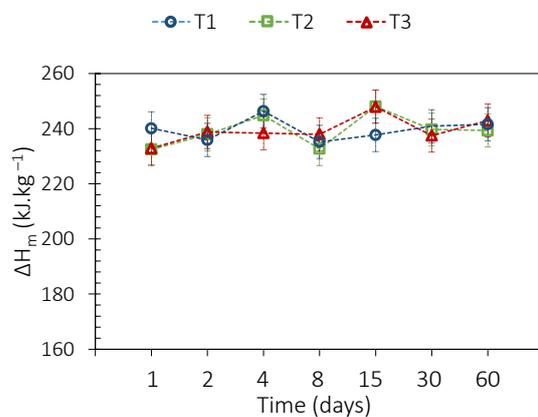
Figure 9. ΔH_m variation of adipic acid.
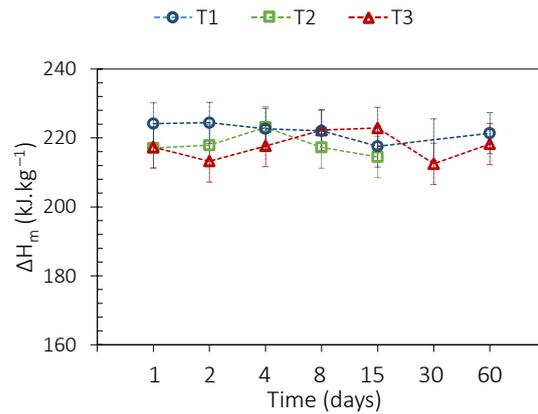
Figure 10. ΔH_m variation of sebacic acid.

3.3. PCM and Envelope Thermal Aging

The same measurements of T_{onset} and ΔH_m were conducted on sebacic and adipic acids in contact with stainless steel 316L or steel P265GH, respectively, shown in Figures 11–14 with steel corrosion speed depicted in Figures 15–19 with steel corrosion speed depicted in Figure 20. In each graph, T1, T2, and T3 are the above-mentioned aging temperatures. The steel samples were immersed from 1 to 60 days in the melted PCM.
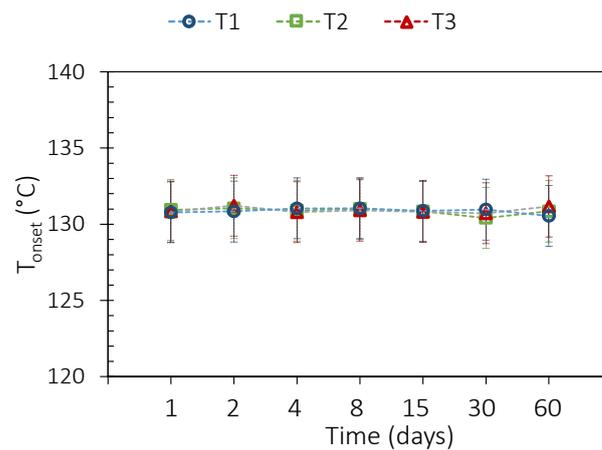
Figure 11. T_{onset} variation of sebacic acid aged with 316L.
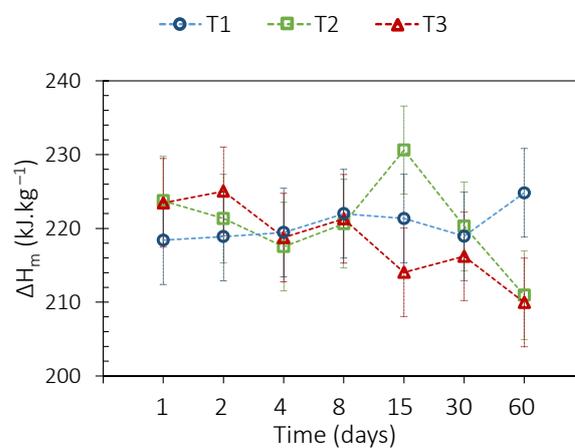
Figure 12. ΔH_m variation of sebacic acid aged with 316L.
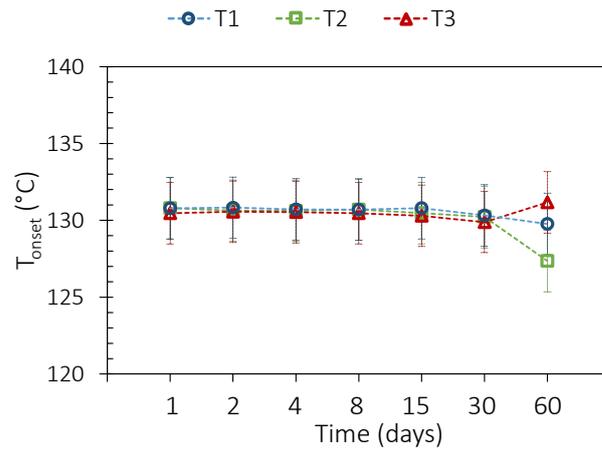
Figure 13. T_{onset} variation of sebacic acid aged with P265GH.
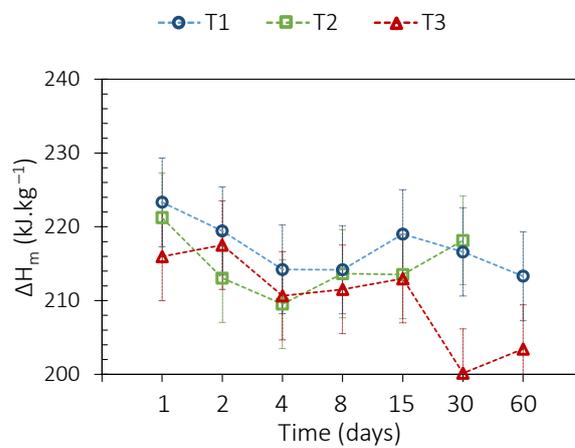
Figure 14. ΔH_m variation of sebacic acid aged with P265GH.
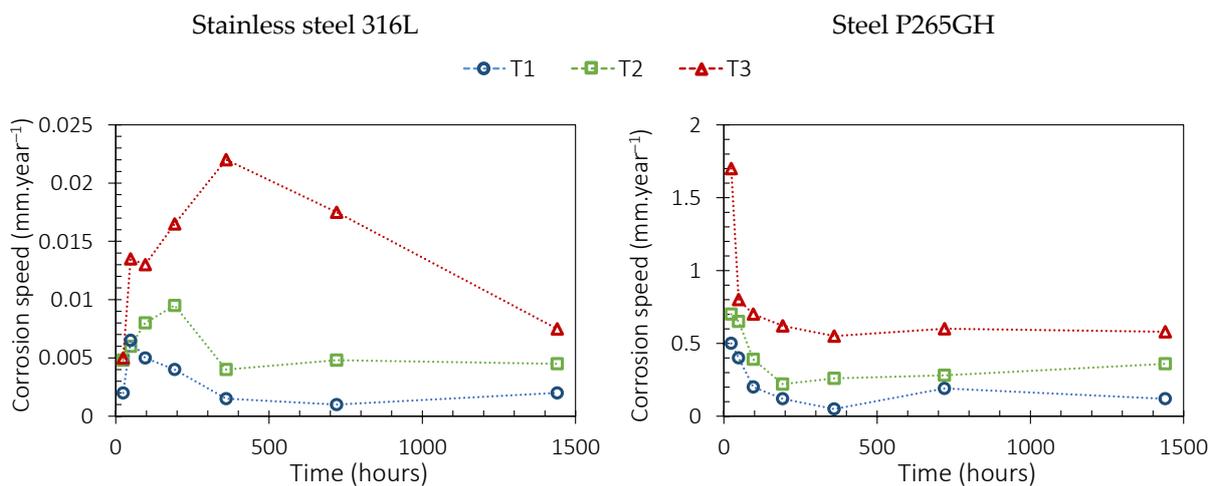
Figure 15. Corrosion kinetics of stainless steel 316L (**left**) and steel P265GH (**right**) in contact with sebacic acid at 3 different temperatures (T1 = 146 °C, T2 = 156 °C, and T3 = 166 °C).
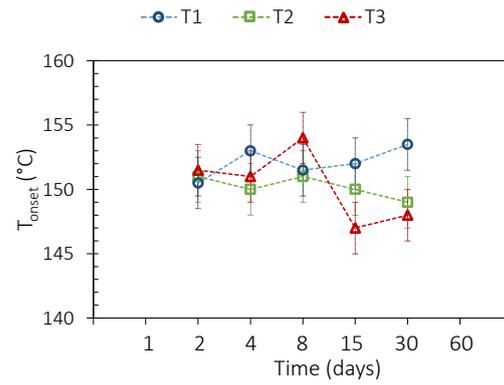
Figure 16. T_{onset} variation of adipic acid aged with 316L.
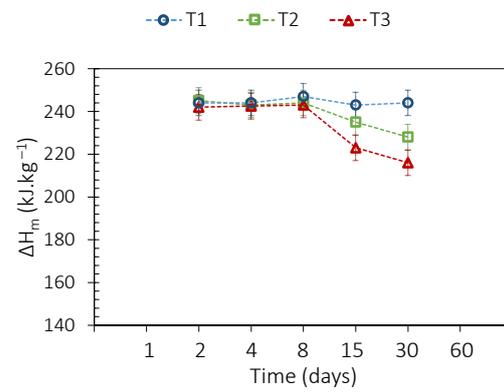
Figure 17. ΔH_m variation of adipic acid aged with 316L.
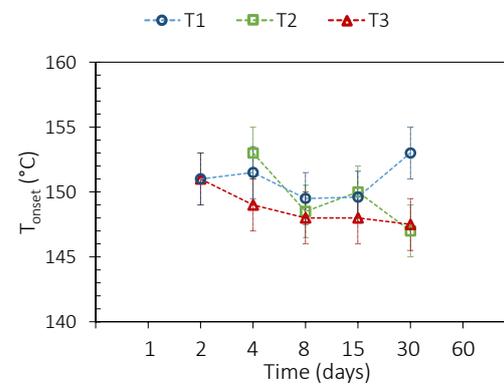
Figure 18. T_{onset} variation of adipic acid aged with P265GH.
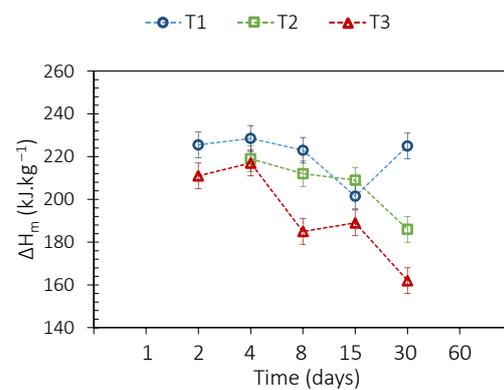
Figure 19. ΔH_m variation of adipic acid aged with P265GH.
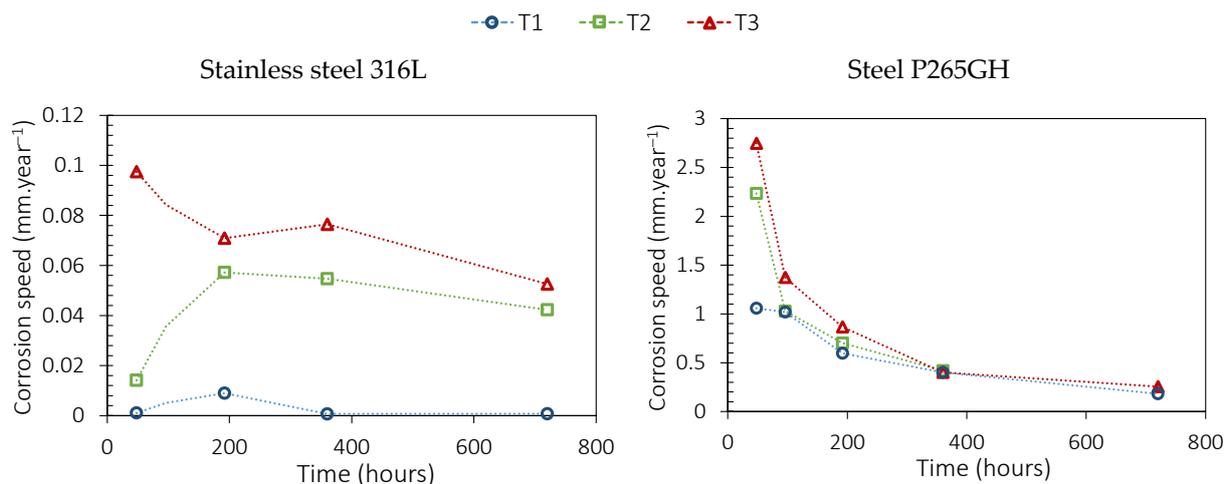
Figure 20. Corrosion kinetics of stainless steel 316L (**left**) and steel P265GH (**right**) in contact with adipic acid at 3 different temperatures (T1 = 166 °C, T2 = 176 °C, and T3 = 186 °C).

3.3.1. Sebacic Acid

The sebacic acid T_{onset} remained stable either when the PCM was in contact with 316L (Figure 11) or P265GH (Figure 13). The latent heat of fusion seemed to be more affected: at T3 = 166 °C (35 °C above the PCM onset temperature), small drops of 5% and 10% were observed, respectively, for 316L (Figure 12) and P265GH (Figure 14). However, the stability considering ΔH_m evolution was better at lower temperatures, and the industrial use of sebacic acid should be validated under T1 = 146 °C (15 °C above the PCM onset temperature) without restrictions for 316L and with vigilance for P265GH.

The corrosion speed (Equation (1)) also worsened when the aging temperature increased (Figure 15). A constant value was reached after ~400 h, except for the stainless steel sample immersed in the PCM at T3 that required more than 1400 h to stabilize. Concerning the stainless steel samples, a satisfying value below 0.02 mm·year^{-1} was attained at all temperatures, satisfying the recommendations from Table 3 for long-term use. Conversely, the P265GH steel samples showed corrosion speeds above 0.1 mm·year^{-1} even at the lower temperatures, impeding its long-term use in the targeted environment.

3.3.2. Adipic Acid

The investigated thermal properties of adipic acid maintained a stable value when it was in contact either with 316L or P265GH at the lower temperature T1 = 166 °C (15 °C above the PCM onset temperature). However, the temperature increase had a noticeably damaging effect on those properties. The T_{onset} fell up to 4 °C at T2 = 176 °C and T3 = 186 °C for both steels (Figures 16 and 18). This ~2.5% variation could be acceptable if it tended to stabilize, which could be established by longer experiments. The latent heat of fusion appears to start a decrease which limits cannot be estimated after 2 months of thermal aging (Figures 17 and 19). Between the initial measurement and the 30th day value, this property lost at T2 and T3, respectively, 7% and 11% of its value for the pair PCM/316L and 24% and 33% of its value for the pair PCM/P265GH. Thus, the adipic acid should be used preferably below T1 = 166 °C in the targeted exchanger.

As depicted in Figure 20, the corrosion speed of 316L is far below the recommendations at T1 = 166 °C, and suitable for careful use at 176 °C and 186 °C. The corrosion speed plateau was not reached for these last two temperatures, and the final value should be even closer to the recommended rank. As for the steel P265GH, the corrosion speed is likely to stabilize around 0.2 mm·year^{-1} for all three temperatures, meaning this material is not appropriate in long-term use for this application.

4. Conclusions

This work aimed to identify suitable phase change materials (PCMs) for waste heat recovery and reuse between 120 °C and 150 °C, the temperature range with an underexploited high-volume potential. Thirty-two PCMs in this temperature range were evaluated on criteria from the literature: thermal stability, non-toxicity, minimal enthalpy variation (more than 50 kWh·m^{-3}), cost (ideally less than 100 EUR·KWh^{-1}), and industrial availability. This reduced the list to six candidates: succinic anhydre acid, benzoic acid, phtalic acid, sebacic acid, dimethyl terephthalate, and adipic acid.

These materials' cycling behavior and thermal damage were studied by calorimetry and thermogravimetry. The succinic anhydre acid, the benzoic acid, the phtalic acid, and the dimethyl terephthalate showed a mass loss higher than 1% at temperatures close to, or even below, the melting temperature (less than 2 °C difference). They consequently were considered ill fitted for industrial use. The two remaining candidates' (sebacic and adipic acid) ability to conserve their properties when submitted to punctual temperature increases were tested by a thermal aging study: the PCMs were exposed to temperatures above 15 °C, 25 °C, and 35 °C to their melting temperatures during 1 to 60 days. No noticeable degradation was revealed by the regular thermo-physical property characterization (T$_{onset}$ and ΔH$_m$) when they were aged alone. Then, their compatibility with the envelope materials (stainless steel 316L and steel P265GH) were evaluated through the same PCM thermal aging campaign, now with enveloping samples immersed in the liquid. The steel P265GH caused a degradation of the PCM latent heat of fusion, especially as to adipic acid, and corroded at a speed not suitable for long-term use according to industrial recommendations. This steel should then be replaced from the exchanger to ensure satisfying performances of the thermal storage system through its lifetime. The use of the stainless steel 316L fit with the corrosion recommendations and the conservation of thermal properties for both PCMs, but the operating conditions should not exceed a temperature of 15 °C above the melting temperature.

Now that the MCP has been selected, it needs to be integrated into the storage system (heat exchanger). The combination of this material with the selected heat exchanger design must be tested to ensure that it is suitable for real applications. Essentially, this will involve checking whether the storage system delivers the expected power.

Author Contributions: Investigation, S.R. and Y.L.; writing—original draft preparation, Y.L.; writing—review and editing, supervision, D.H. and J.-P.B. All authors have read and agreed to the published version of the manuscript.

Data Availability Statement: Dataset available on request from the authors.

References

1. ADEME. Chaleur Fatale, La Librairie ADEME. 2017. Available online: https://librairie.ademe.fr/energies-renouvelables-reseaux-et-stockage/2312-chaleur-fatale-9791029708954.html (accessed on 2 September 2023).
2. Papapetrou, M.; Kosmadakis, G.; Cipollina, A.; La Commare, U.; Micale, G. Industrial waste heat: Estimation of the technically available resource in the EU per industrial sector, temperature level and country. *Appl. Therm. Eng.* **2018**, *138*, 207–216. [CrossRef]
3. Johnson, I.; Choate, W.T.; Davidson, A. *Waste Heat Recovery. Technology and Opportunities in U.S. Industry*; US Department of Energy: Washington, DC, USA, 2008. [CrossRef]
4. López-Sabirón, A.M.; Aranda-Usón, A.; Ferreira, V.J.; Ferreira, G. Environmental profile of latent energy storage materials applied to industrial systems. *Sci. Total Environ.* **2014**, *473–474*, 565–575. [CrossRef]
5. Daniarta, S.; Nemś, M.; Kolasiński, P. A review on thermal energy storage applicable for low- and medium-temperature organic Rankine cycle. *Energy* **2023**, *278*, 127931. [CrossRef]
6. Zalba, B.; Marin, J.; Cabeza, L.F.; Mehling, H. Review on thermal energy storage with phase change: Materials, heat transfer analysis and applications. *Appl. Therm. Eng.* **2003**, *23*, 251–283. [CrossRef]
7. Abhat, A. Low temperature latent heat thermal energy storage: Heat storage materials. *Sol. Energy* **1983**, *30*, 313–332. [CrossRef]

8. Sharma, R.K.; Ganesan, P.; Tyagi, V.V.; Metselaar, H.S.C.; Sandaran, S.C. Developments in organic solid–liquid phase change materials and their applications in thermal energy storage. *Energy Convers. Manag.* **2015**, *95*, 193–228. [CrossRef]
9. Gunasekara, S.N.; Pan, R.; Chiu, J.N.; Martin, V. Polyols as phase change materials for surplus thermal energy storage. *Appl. Energy* **2016**, *162*, 1439–1452. [CrossRef]
10. Beaupere, N.; Soupremanien, U.; Zalewski, L. Nucleation triggering methods in supercooled phase change materials (PCM), a review. *Thermochim. Acta* **2018**, *670*, 184–201. [CrossRef]
11. Lin, Y.; Jia, Y.; Alva, G.; Fang, G. Review on thermal conductivity enhancement, thermal properties and applications of phase change materials in thermal energy storage. *Renew. Sustain. Energy Rev.* **2018**, *82*, 2730–2742. [CrossRef]
12. Vasu, A.; Hagos, F.Y.; Noor, M.M.; Mamat, R.; Azmi, W.H.; Abdullah, A.A.; Ibrahim, T.K. Corrosion effect of phase change materials in solar thermal energy storage application. *Renew. Sustain. Energy Rev.* **2017**, *76*, 19–33. [CrossRef]
13. Krishna, D.J.; Shinde, A. Step by Step Methodology for the Assessment of Metal Corrosion Rate with PCMs Suitable for Low Temperature Heat Storage Applications. *Mater. Today Proc.* **2017**, *4*, 10039–10042. [CrossRef]
14. Moreno, P.; Miró, L.; Solé, A.; Barreneche, C.; Solé, C.; Martorell, I.; Cabeza, L.F. Corrosion of metal and metal alloy containers in contact with phase change materials (PCM) for potential heating and cooling applications. *Appl. Energy* **2014**, *125*, 238–245. [CrossRef]
15. Oró, E.; Miró, L.; Barreneche, C.; Martorell, I.; Farid, M.M.; Cabeza, L.F. Corrosion of metal and polymer containers for use in PCM cold storage. *Appl. Energy* **2013**, *109*, 449–453. [CrossRef]
16. Yin, Y.; Rumman, R.; Chambers, B.A.; Liu, M.; Jacob, R.; Belusko, M.; Bruno, F.; Lewis, D.A.; Andersson, G.G. Corrosion interface formation in thermally cycled stainless steel 316 with high-temperature phase change material. *Sol. Energy Mater. Sol. Cells* **2021**, *225*, 111062. [CrossRef]
17. Delise, T.; Tizzoni, A.C.; Ferrara, M.; Corsaro, N.; D'Ottavi, C.; Sau, S.; Licoccia, S. Thermophysical, environmental, and compatibility properties of nitrate and nitrite containing molten salts for medium temperature CSP applications: A critical review. *J. Eur. Ceram. Soc.* **2019**, *39*, 92–99. [CrossRef]
18. Opolot, M.; Zhao, C.; Liu, M.; Mancin, S.; Bruno, F.; Hooman, K. A review of high temperature (≥500 °C) latent heat thermal energy storage. *Renew. Sustain. Energy Rev.* **2022**, *160*, 112293. [CrossRef]
19. Zhou, C.; Wu, S. Medium- and high-temperature latent heat thermal energy storage: Material database, system review, and corrosivity assessment. *Int. J. Energy Res.* **2018**, *43*, 621–661. [CrossRef]
20. Devanuri, J.K.; Gaddala, U.M.; Kumar, V. Investigation on compatibility and thermal reliability of phase change materials for low-temperature thermal energy storage. *Mater. Renew. Sustain. Energy* **2020**, *9*, 24. [CrossRef]
21. Ferrer, G.; Solé, A.; Barreneche, C.; Martorell, I.; Cabeza, L.F. Corrosion of metal containers for use in PCM energy storage. *Renew. Energy* **2015**, *76*, 465–469. [CrossRef]
22. Kahwaji, S.; Johnson, M.B.; Kheirabadi, A.C.; Groulx, D.; White, M.A. Fatty acids and related phase change materials for reliable thermal energy storage at moderate temperatures. *Sol. Energy Mater. Sol. Cells* **2017**, *167*, 109–120. [CrossRef]
23. Hua, W.; Xu, X.; Zhang, X.; Yan, H.; Zhang, J. Progress in corrosion and anti-corrosion measures of phase change materials in thermal storage and management systems. *J. Energy Storage* **2022**, *56*, 105883. [CrossRef]
24. Calabrese, L.; Brancato, V.; Paolomba, V.; Proverbio, E. An experimental study on the corrosion sensitivity of metal alloys for usage in PCM thermal energy storages. *Renew. Energy* **2019**, *138*, 1018–1027. [CrossRef]
25. Mohamed, S.A.; Al-Sulaiman, F.A.; Ibrahim, N.I.; Zahir, M.H.; Al-Ahmed, A.; Saidur, R.; Yılbaş, B.S.; Sahin, A.Z. A review on current status and challenges of inorganic phase change materials for thermal energy storage systems. *Renew. Sustain. Energy Rev.* **2017**, *70*, 1072–1089. [CrossRef]
26. Sharma, A.; Tyagi, V.V.; Chen, C.R.; Buddhi, D. Review on thermal energy storage with phase change materials and applications. *Renew. Sustain. Energy Rev.* **2009**, *13*, 318–345. [CrossRef]
27. Hauer, A. Thermal Energy Storage, Technology Brief, ETSAP, IRENA. 2013. Available online: https://www.irena.org/-/media/Files/IRENA/Agency/Publication/2013/IRENA-ETSAP-Tech-Brief-E17-Thermal-Energy-Storage.pdf (accessed on 1 September 2023).
28. Espagnet, A.R. Techno-Economic Assessment of Thermal Energy Storage Integration into Low Temperature District Heating Networks. Master's Thesis, KTH School of Industrial Engineering and Management, Stockholm, Sweden, 2016.
29. Lalau, Y.; Haillot, D.; Rigal, S.; Bedecarrats, J.-P. Stockage Thermique Latent Pour la Récupération de Chaleur Fatale (120–150 °C): Stabilité des Matériaux. In *Annales du Congrès Annuel de la Société Française de Thermique 2020*; Tome 1; Societe Francaise de Thermique: Strasbourg, France, 2020; pp. 145–152.
30. Jankowski, N.R.; Mccluskey, F.P. A review of phase change materials for vehicle component thermal buffering. *Appl. Energy* **2014**, *113*, 1525–1561. [CrossRef]
31. Waschull, J.; Müller, R.; Römer, S. Investigation of Phase Change Materials for Elevated Temperatures; Dresden, Germany. 2009. Available online: https://www.researchgate.net/publication/309045719_Investigation_of_phase_change_materials_for_elevated_temperatures (accessed on 4 September 2023).
32. Sharma, S.D.; Sagara, K. Latent Heat Storage Materials and Systems: A Review. *Int. J. Green Energy* **2005**, *2*, 1–56. [CrossRef]
33. Haillot, D.; Bauer, T.; Kröner, U.; Tamme, R. Thermal analysis of phase change materials in the temperature range 120–150 °C. *Thermochim. Acta* **2011**, *513*, 49–59. [CrossRef]
34. Sharma, S.D.; Kitano, H.; Sagara, K. Phase Change Materials for Low Temperature Solar Thermal Applications. *Res. Rep. Fac. Eng. Mie Univ.* **2004**, *29*, 31–64.

35. Nazir, H.; Batool, M.; Osorio, F.J.B.; Isaza-Ruiz, M.; Xu, X.; Vignarooban, K.; Phelan, P.; Kannan, A.M. Recent developments in phase change materials for energy storage applications: A review. *Int. J. Heat Mass Transf.* **2019**, *129*, 491–523. [CrossRef]
36. Dumas, J.-P. Etude de la Rupture de Métastabilité et du Polymorphisme de Corps Organiques. Ph.D. Thesis, Université de Pau, Pau, France, 1976.
37. Kouadio, T.; Sommier, A. Characterization of different sugar alcohols as phase change materials for thermal energy storage applications. *Sol. Energy Mater. Sol. Cells* **2017**, *159*, 560–569.
38. Da Cunha, J.P.; Eames, P. Thermal energy storage for low and medium temperature applications using phase change materials–A review. *Appl. Energy* **2016**, *177*, 227–238. [CrossRef]
39. Huang, Z.; Xie, N.; Luo, Z.; Gao, X.; Fang, X.; Fang, Y. Characterization of medium-temperature phase change materials for solar thermal energy storage using temperature history method. *Sol. Energy Mater. Sol. Cells* **2018**, *179*, 152–160. [CrossRef]
40. Tan, P.; Brütting, M.; Vidi, S.; Ebert, H.-P.; Johansson, P.; Kalagasidis, A.S. Characterizing phase change materials using the T-History method: On the factors influencing the accuracy and precision of the enthalpy-temperature curve. *Thermochim. Acta* **2018**, *666*, 212–228. [CrossRef]
41. Gibout, S.; Franquet, E.; Haillot, D.; Bédécarrats, J.-P.; Dumas, J.-P. Challenges of the usual graphical methods used to characterize Phase Change Materials by Differential Scanning Calorimetry. *Appl. Sci.* **2018**, *8*, 66. [CrossRef]
42. *ASTM G1-03(2017)e1*; Standard Practice for Preparing, Cleaning, and Evaluating Corrosion Test Specimens. ASTM International: West Conshohocken, PA, USA, 2017. [CrossRef]
43. Davis, J.R. *Corrosion: Understanding the Basics*; ASM International: West Conshohocken, PA, USA, 2000.